

Preparation and Characterization of a Low-Cost and Environmentally Friendly Epoxy Coating for Concrete Structures Protection



Ansam Neamah Naji^{1*}, Zoalfokkar Kareem Mezaal Al-obad¹, Mohammed H. Al Maamori²

¹ Polymer Engineering and Petrochemical Industries Department, College of Materials Engineering, University of Babylon, Babylon 51001, Iraq

² Prosthetics and Orthotics Engineering, Al-Mustaqbal University College, Babylon 51002, Iraq

Corresponding Author Email: ansamneamah91@gmail.com

Copyright: ©2025 The authors. This article is published by IETA and is licensed under the CC BY 4.0 license (<http://creativecommons.org/licenses/by/4.0/>).

<https://doi.org/10.18280/acsm.490511>

ABSTRACT

Received: 14 August 2025

Revised: 19 October 2025

Accepted: 24 October 2025

Available online: 31 October 2025

Keywords:

epoxy resin, concrete waste, cement kiln dust (CKD), mechanical properties (Tensile, hardness, impact, fracture toughness (SENB, CT) and pull off adhesion test)

This investigation focused on the development of a sustainable and cost-effective epoxy-based coating system tailored for the protection of concrete infrastructure. The epoxy matrix was reinforced with recycled industrial by-products—namely concrete waste (CW) and cement kiln dust (CKD)—incorporated at loadings of 2–10 wt%. Specimen fabrication was carried out using an industrially scalable mixing protocol to ensure practical applicability. Mechanical characterization revealed that CW reinforcement markedly enhanced tensile performance, achieving a peak strength of 54 MPa at 6 wt% CW, compared to 18.5 MPa for the unmodified epoxy, although higher filler loadings induced a decline due to agglomeration phenomena. In contrast, CKD incorporation did not result in a comparable tensile improvement. The modulus of elasticity exhibited a substantial increase, rising from 0.62 GPa in the neat epoxy to 1.363 GPa at 4 wt% CW and 0.48 GPa at 8 wt% CKD. Surface hardness, measured by Shore D, increased progressively, reaching 80.9 at 8 wt% CW and 81.6 at 6 wt% CKD. Impact resistance was similarly improved, attaining values of 5.26 kJ/m² at 4 wt% CW and 5.89 kJ/m² at 2 wt% CKD. Single-edge notched bending (SENB) tests indicated that fracture toughness was maximized at 0.2067 MPa·m^{1/2} for 4 wt% CW and 0.1677 MPa·m^{1/2} for 2 wt% CKD. Adhesion strength improvements at intermediate filler contents were attributed to effective mechanical interlocking, as corroborated by SEM analysis, while FTIR spectra suggested predominantly physical interactions within the composite system.

1. INTRODUCTION

In recent years, significant advancements have been made in the development of specialty polymers, particularly to meet the growing demands of the construction sector. This progress aligns with the increasing global emphasis on environmental preservation and the reduction of industrial pollution, which has, in turn, driven the adoption of recycled materials and heightened the focus on cost-efficiency in material selection and processing [1].

In the construction sector, epoxy-based systems serve dual preventive and restorative functions, being extensively utilized in protective coatings, repair mortars, and sanitation applications. Beyond their structural and functional roles, such systems also enhance the aesthetic quality of surfaces, particularly in industrial flooring applications [2]. Among polymeric materials, epoxy resins have achieved broad industrial adoption as coatings, adhesives, and lightweight structural components due to their outstanding combination of high mechanical strength, superior chemical resistance, and excellent adhesion to diverse substrates [3]. Within the industrial construction domain, epoxy coatings are especially valued for imparting surfaces with exceptional resistance to

aggressive chemicals and persistent contaminants. However, the widespread application of epoxy resins is constrained by their relatively high cost [4]. Accordingly, considerable research has been directed toward the incorporation of alternative additives and fillers to partially substitute the resin and curing agents, with the aim of reducing material costs while retaining or enhancing performance characteristics [5]. In this regard, recycled materials such as concrete waste and Portland cement have emerged as promising candidates. Their incorporation not only augments the mechanical and adhesive behavior of polymeric matrices but also contributes to environmental sustainability by valorizing construction debris, a critical source of ecological burden [6]. For instance, Almusallam et al. [7] reported superior adhesion strength (3.3 MPa after two weeks in single-layer application) for epoxy coatings compared with polyurethane and acrylic systems, in addition to remarkable crack-healing capacity, thermal stability, and resistance to chloride ingress. Similarly, Szewczak and Łagód [8] emphasized that epoxy resins demonstrate excellent chemical and water resistance, along with strong interfacial bonding to concrete and steel substrates, where the inclusion of fillers further enhanced durability and protective efficiency. Moreover, the intrinsically low

shrinkage during curing promotes dimensional stability and structural integrity of the coating layers [9]. Consequently, epoxy coatings remain a material of choice for harsh service environments, and recent research trends have focused on their cost reduction and functional enhancement through the integration of conventional or sustainable fillers derived from industrial and construction by-products [10, 11].

Concrete surface coating has emerged as a widely adopted technique for the rehabilitation of deteriorated structures; however, its long-term effectiveness is primarily governed by the coating's adhesion strength to the concrete substrate and its resistance to chemically aggressive environments. Previous investigations have demonstrated that polymeric systems—particularly epoxy-based coatings—offer superior protection for concrete exposed to acidic media, such as 3% sulfuric acid solutions, owing to their excellent chemical resistance and strong interfacial bonding. The durability of such protective systems is strongly influenced by multiple parameters, including the intrinsic chemical composition of the coating, the application methodology, and the surface condition of the concrete substrate, all of which collectively dictate the overall performance [12].

In this context, cement kiln dust (CKD), a fine particulate by-product of cement manufacturing, has attracted increasing research interest. Although CKD exhibits physical properties comparable to those of Portland cement, it is predominantly regarded as industrial waste and typically disposed of in landfills [13]. Recent studies, however, have highlighted its potential as a cost-effective filler in epoxy matrices, demonstrating improvements in thermal stability and performance of the resin, alongside a reduction in overall production costs. This valorization not only mitigates environmental burdens but also supports the development of sustainable, high-performance composite materials [14].

Accordingly, the present study aims to formulate environmentally sustainable and economically viable epoxy-based coatings for the protection of concrete structures. Particular emphasis is placed on evaluating the influence of

incorporating recycled concrete waste (CW) and cement kiln dust (CKD), at varying weight fractions, on the mechanical, thermal, and protective performance of epoxy coatings.

2. EXPERIMENTAL PART

2.1 Materials used

2.1.1 Epoxy resin

The epoxy resin used in this study, Strong coat 400, was purchased from DCP Company, located in Hilla, Iraq. It is a two-component system comprising a resin and a hardener.

2.1.2 Waste concrete

Waste concrete generally contains sand, gravel, and various aggregates. When crushed and processed into fine particles with a size of 125 μm or smaller, it can serve effectively as a filler material, helping to reduce environmental pollution and lower construction costs.

2.1.3 Cement kiln dust (CKD)

Cement kiln dust, a fine powder sieved to 125 μm , was sourced from the Karbala Cement Factory in Iraq. It was used as a filler in epoxy resin to enhance properties, reduce costs, and support sustainable construction.

2.2 Preparation of pure epoxy samples

The epoxy resin was mixed with the hardener at a weight ratio of 85:15 and stirred mechanically for 5 minutes to achieve a uniform mixture. It was then placed under vacuum at room temperature for 30 minutes to eliminate any entrapped air bubbles. The degassed mixture was poured into a pre-prepared silicone rubber mold and left at room temperature for 24 hours, followed by an additional 7 days to ensure complete curing [15]. The preparation process is shown in Figure 1.

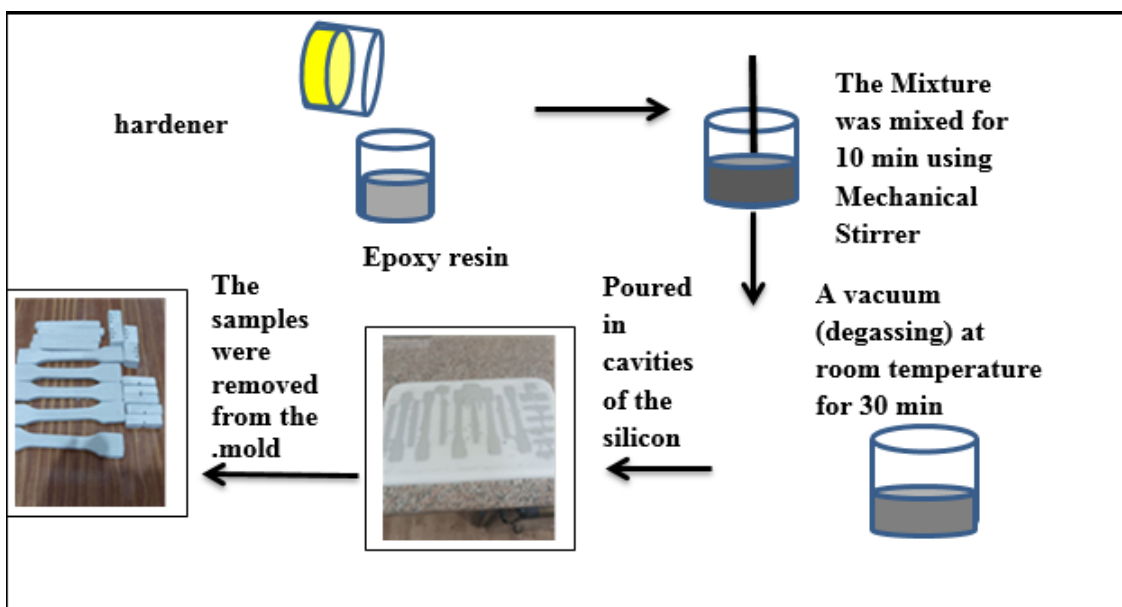


Figure 1. The procedure preparation samples of epoxy pure

2.3 Preparation of waste concrete particles

As shown in Figure 2, it was taken a ready-made concrete

cube was processed through several steps. First, it was cleaned with water, then dried using both room temperature and an oven at 80°C. The dried concrete was ground with a mortar

until it became a fine powder. The powder was then sieved to separate coarse particles, using a 125 µm mesh to obtain the fine particles suitable for use in the epoxy resin [16]. Composite samples were then prepared by incorporating different weight percentages of waste concrete particles (0%, 2%, 4%, 6%, 8%, and 10%wt) into the epoxy resin.

2.4 Preparation of composite samples

Composite samples of epoxy resin /concrete waste (EP/CW) and epoxy resin / cement kiln dust (EP/CKD) were prepared by incorporating varying proportions (2%, 4%, 6%,

8%, and 10%wt) of waste concrete particles and cement kiln dust as fillers into the epoxy resin. The fillers were first mixed with the resin using a mechanical stirrer for 30 minutes to ensure uniform dispersion. Subsequently, the hardener was added and the mixture stirred for an additional 5 minutes. The resulting mixture was then subjected to vacuum degassing for 30 minutes to eliminate entrapped air bubbles. Finally, the mixture was poured into a pre-prepared silicone rubber mold and left at room temperature for 24 hours, followed by an additional 7 days to ensure complete curing, as illustrated in Figure 3.



Figure 2. Steps of preparing powder concrete waste

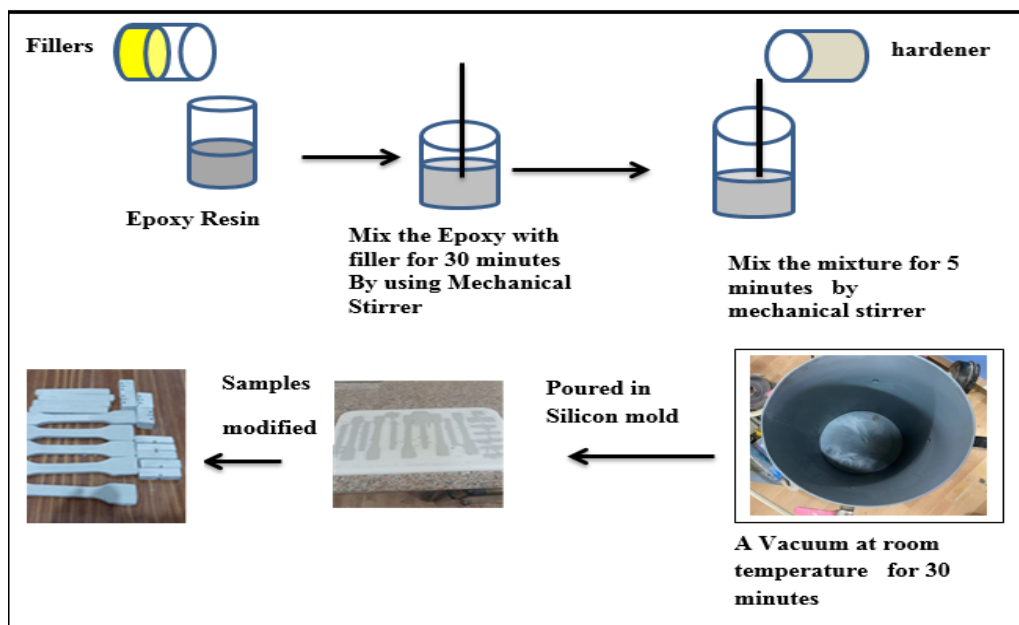


Figure 3. The procedure for preparing samples of the composite epoxy coating

2.5 Experimental tests

2.5.1 Tensile strength test

Tensile tests were conducted at room temperature using a microcomputer-controlled electronic universal testing machine (Model WDW-5E, China) with a load capacity of 5 KN and a testing speed of 5 mm/min, following the ISO 75-1 standard [17]. The tests were performed in the laboratory of the College of Materials Engineering, University of Babylon. Multiple specimens were prepared and tested under identical conditions, as illustrated in Figure 4. Each specimen was subjected to uniaxial tensile loading until failure, and the corresponding stress–strain curves were recorded for analysis. The tensile strength and modulus were calculated using the following equations [18]:

$$\sigma = \frac{F}{A} \quad (1)$$

$$E = \frac{\Delta\sigma}{\Delta\varepsilon} \quad (2)$$

where:

σ : Tensile strength (MPa).

E: Elastic modulus (MPa).

F: Load (N).

A: Cross-sectional area of sample (mm²).

$\Delta\sigma = \sigma_2 - \sigma_1$ Stress of sample (MPa).

$\Delta\varepsilon = \varepsilon_2 - \varepsilon_1$ Strain of sample.



Figure 4. Specimens of the tensile test

2.5.2 Hardness (Shore D) test

The hardness test is a fundamental method for assessing a material's resistance to localized deformation and is critical in evaluating the durability and surface integrity of coatings. In this study, hardness measurements were conducted following the ASTM D2240 standard [19]. A standard Shore D hardness tester equipped with a sharp indenter was used to evaluate the surface hardness of the samples, which included pure epoxy (EP), epoxy with concrete waste (EP/C), and epoxy with cement kiln dust (EP/CKD). For each sample, measurements were taken at six different points on the surface, and the final hardness value was determined as the average of these six readings.

2.5.3 Impact strength test

The pendulum impact test is one of the most widely used methods for evaluating the impact resistance of plastic materials. In this study, specimens were prepared under ISO 179-1 [20]. Multiple specimens were tested for each composition ratio. Figure 5 illustrates both standard and experimental un-notched specimens.

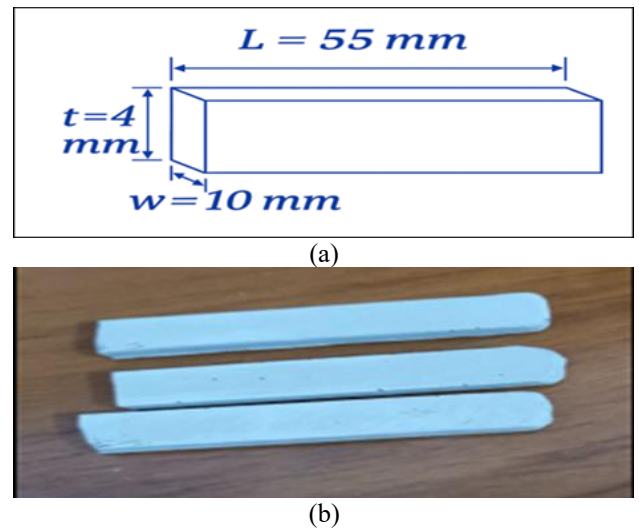


Figure 5. (a) Schematic impact specimen, (b) experimental impact specimens

During testing, each specimen was clamped in a cantilever position and struck by the pendulum's arm. The energy absorbed by the specimen during fracture is referred to as the breaking energy [21], and it was measured in joules. The impact strength was then calculated based on the energy required to break the specimen, using the following equation [20]:

$$Gc = Uc / A \quad (3)$$

where:

Gc is impact strength (J/m²).

Uc is energy of impact (J).

A is an abbreviation representing the cross-sectional area (m²).

2.5.4 Fracture toughness tests

For the fracture toughness tests, the Compact Tension (CT) and Single Edge Notched Beam (SENB) methods were employed. Following the specimen preparation process, a sharp crack was introduced at the center of the pre-existing notch using a razor blade [15]. This was achieved by applying a specific weight combined with manual pressure (referred to as "hand force") to generate a precise incision, as illustrated in Figure 6. This technique, commonly adopted in various studies, produces a sharp crack approximately 1 mm in length, serving as a stress concentrator.

2.5.5 Compact tension (C.T) test

The fracture toughness test was performed at room temperature by ASTM D5045 [22]. A universal testing machine (Model WDW/5E) was utilized for this purpose.

To evaluate the fracture toughness characteristics, the test was conducted at a constant crosshead speed of 5 mm/min using a 5 KN load cell. The stress intensity factor K_{Ic} , representing the material's fracture toughness under plane strain conditions, was calculated using the following equation [23]:

$$K_{Ic} = \left(\frac{P_{max}}{b\sqrt{w}} \right) F \left(\frac{a}{w} \right) \quad (4)$$

$$f\left(\frac{a}{w}\right) = \frac{\left(2 + \frac{a}{w}\right) \left[0.886 + 4.64 \left(\frac{a}{\pi}\right) - 13.32 \left(\frac{a}{w}\right)^2 + 14.72 \left(\frac{a}{w}\right)^3 - 5.6 \left(\frac{a}{\pi}\right)^4 \right]}{\left(1 - \frac{a}{w}\right)^{3/2}} \quad (5)$$

where,

P max: the maximum load, b: thickness of sample, W: the width, a: the initial crack length, $X = \frac{a}{w}$, where $(0 < x < 1)$.

2.5.6 SENB test

The Single Edge Notched Beam (SENB) test was conducted to evaluate the fracture toughness of the micro-composite specimens. Testing was performed using a universal testing machine (Model WDW/5E), with the specimens configured as shown in Figure 7. The test was carried out at room temperature following ASTM D5045 [22]. A constant crosshead speed of 5mm/min and a span length of 40 mm were maintained throughout the test. The stress intensity factor (K_{IC}), indicative of fracture toughness under plane strain conditions, was calculated using the equations provided in the reference [24].

$$K_{IC} = \left(\frac{P}{BW^{3/2}}\right) f\left(\frac{a}{w}\right) \quad (6)$$

$$f(x) = 6x^{1/2} \frac{[1.99 - x(1-x)(2.15 - 3.93x + 2.7x^2)]}{(1+2x)(1-x)^{3/2}} \quad (7)$$

$Gc = Uc / A$

where $(0 < x < 1)$, P is the critical load for split propagation, B is the specimen thickness, W is the specimen width, a is the crack length, and f(x) is a non-dimensional shape factor with

$x = a/w$.

2.5.7 Adhesion strength (pull off) test

The pull-off adhesion test, conducted under ASTM D4541 [24] as seen in Figure 8, involves cutting through the coating layer down to the surface of the concrete substrate using a circular area equal in diameter to that of the loading fixture (dolly or stud). The fixture is then bonded perpendicularly to the coating surface using an appropriate adhesive. Following proper curing, tensile load is applied normal to the surface until failure occurs. The pull-off strength is determined using the equation [25]:

$$A = 4 F / \pi d^2 \quad (8)$$

where,

A is the pull-off strength at failure (MPa), F is the peak force applied at failure (N), and d is the diameter of the loading fixture (mm).

2.5.8 Fourier transform infrared spectrometer (FTIR) test

The FTIR test was performed using a SHIMADZU IR Affinity-1 spectrometer (Japan), equipped with a mid-IR source ($400-4000 \text{ cm}^{-1}$), DTGS detector, and KBr beam splitter. According to ASTM E1252 [26]. A small amount of the sample was ground, mixed with potassium bromide (99% ratio), and pressed into a semi-transparent disc to allow infrared radiation penetration. This analysis was conducted to investigate the nature of the bond, physical or chemical, between the epoxy matrix and fillers in epoxy, EP/CW, and EP/CKD composites.

2.5.9 Scanning electron microscopy (SEM)

Scanning electron microscopy (SEM) is a powerful technique used for observing and characterizing the surface morphology of both organic and inorganic materials. It provides critical data regarding the topography and structural features of the sample. In the present study, SEM was employed to investigate the dispersion and distribution of fillers within the epoxy resin matrix. The analysis was conducted using the (Axia ChemiSEM) device.

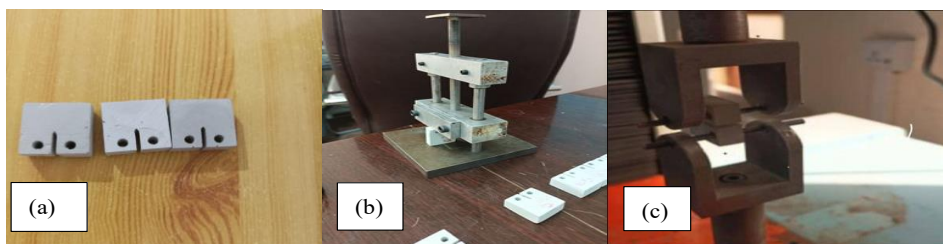


Figure 6. (a) Image of the compact fracture sample, (b) Introduction of the pre-crack incision, (c) Compact tension (CT) testing setup

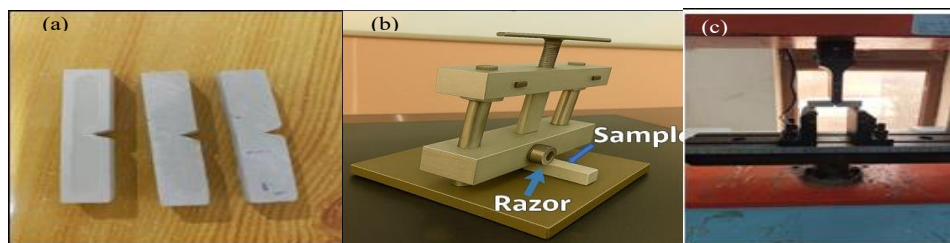


Figure 7. (a) Specimens prepared for fracture toughness testing, (b) Creation of the V-shaped notch (crack) in the SENB samples, (c) Fracture toughness test



Figure 8. The three stages: (a) preparation of the concrete specimen with bolts, (b) during tensile testing apparatus, and (c) specimens after testing with bolts removed

3. RESULTS AND DISCUSSIONS

3.1 Tensile results

Figure 9 presents a comparison of the tensile strength values for pure epoxy (EP Pure), epoxy reinforced with varying weight percentages of concrete waste (CW), and epoxy reinforced with cement kiln dust (CKD). The test aimed to evaluate the effect of filler type and loading percentage on the mechanical behavior of the composites and to identify the optimum composition for maximum tensile performance.

The epoxy reinforced with concrete waste exhibited a noticeable improvement in tensile strength with increasing filler content up to 6 wt.%, reaching a peak value of 54 MPa as compared to pure epoxy of 18.5 MPa. The strength increases progressively at 2 wt.% and 4 wt.% (about 37.5 MPa and 50 MPa, respectively), indicating that the inclusion of concrete waste enhances stress transfer and filler-matrix interaction. However, beyond 6 wt.%, a decline in tensile strength is observed at 8 wt.% and 10 wt.% (about 35.3 MPa and 17 MPa, respectively), which could be attributed to filler agglomeration and poor dispersion within the matrix. Such defects likely lead to stress concentration zones and compromise the composite's structural integrity. Therefore, 6 wt.% concrete waste appears to be the optimal filler content for enhancing tensile strength. In contrast, the epoxy composites incorporating cement kiln dust do not exhibit significant improvements in tensile strength. The measured values ranged from 14 MPa to 11.667 MPa, showing minimal and inconsistent variation across different filler loadings. This suggests weak interfacial bonding between CKD particles and the epoxy matrix, possibly due to unfavorable particle morphology or chemical incompatibility, which limits the material's ability to effectively resist tensile forces.

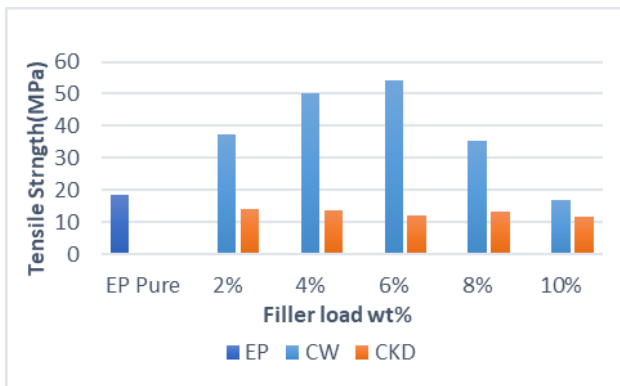


Figure 9. Effect of adding concrete and cement waste (CKD) on the tensile Strength of epoxy coating

Figure 10 presents the effect of incorporating concrete waste and cement kiln dust (CKD) on the elastic modulus of epoxy composites. The addition of concrete waste markedly enhances the stiffness of the epoxy matrix, with a maximum elastic modulus of 1.363 GPa observed at 4 wt.% as compared to pure epoxy of 0.62 GPa. The modulus remains stable at 6 wt.% and 8 wt.%, indicating efficient stress transfer and filler dispersion. However, at 10 wt.%, a significant reduction to 0.61 GPa was recorded, likely due to filler agglomeration and matrix saturation. In contrast, composites containing CKD exhibit inferior performance, with elastic modulus values ranging from 0.34 to 0.48 GPa. These results suggest poor interfacial bonding and inadequate reinforcement efficiency. In some cases, CKD-filled samples performed worse than the neat epoxy, likely due to the formation of internal defects and poor compatibility between CKD particles and the epoxy matrix.

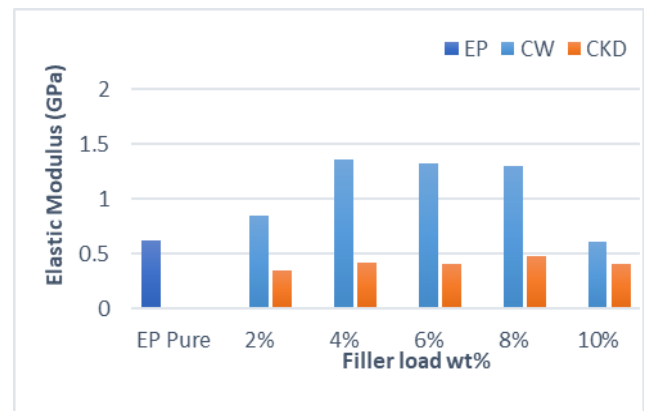


Figure 10. Effect of adding concrete and cement waste (CKD) on the elastic modulus of epoxy coating

3.2 Hardness (Shore D) results

The analysis of the results presented in Figure 11 highlights the influence of incorporating two types of fillers, concrete waste (CW) and cement kiln dust (CKD), on the Shore D hardness of epoxy resin, thereby demonstrating the behavior of the resulting composite in terms of surface resistance to deformation. The results show that pure epoxy has slightly lower hardness. It is noted that the results of all ratios are close to those of pure epoxy. In other words, there is a slight, unnoticeable change in hardness. This is attributed to the physical bonding between the epoxy matrix and the microparticles (as evidenced by the FTIR spectra, which revealed no significant chemical bonding) due to the agglomeration of microparticles within the epoxy matrix.

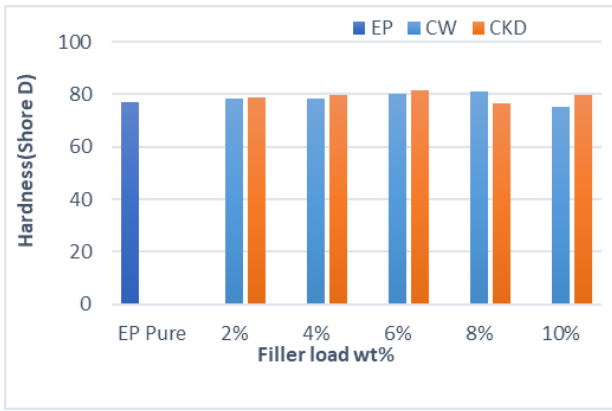


Figure 11. Effect of adding concrete (CW) and cement waste (CKD) on the Hardness (Shore D) of epoxy coating

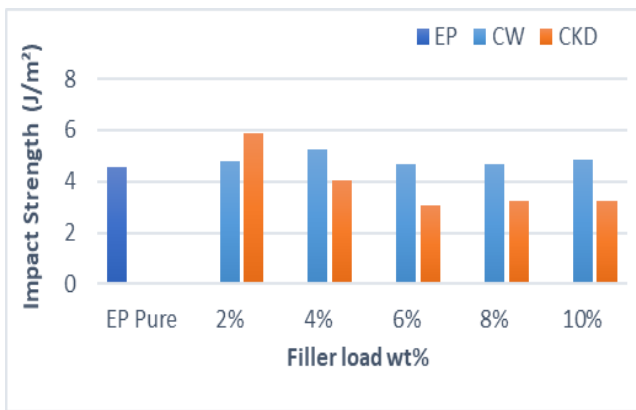


Figure 12. Effect of filler content (wt%) on the impact strength of the epoxy matrix

3.3 Impact strength results

This study investigates the impact of incorporating two types of recycled fillers, concrete waste (CW) and cement kiln dust (CKD), on the fracture resistance (impact strength) of epoxy composites. Filler materials were added at various weight percentages (2%, 4%, 6%, 8%, and 10%) as shown in Figure 12 and fracture energy was selected as the primary performance indicator. The pure epoxy resin (0% filler) served as the reference material and records a fracture energy of 4.56 J/m², reflecting a moderate level of crack resistance in the absence of reinforcement. The addition of concrete waste results in a clear improvement in impact strength, with recorded values of 4.78, 5.26, 4.68, 4.66, and 4.83 J/m² for the 2%, 4%, 6%, 8%, and 10% samples, respectively. The highest value is achieved at 4% filler content (5.26 J/m²), which is attributed to the uniform dispersion of filler particles and their ability to inhibit crack growth, thereby enhancing fracture resistance. At higher contents, the performance remained relatively stable, indicating good compatibility between the filler and the epoxy matrix. In contrast, CKD-filled samples exhibit the highest fracture energy at a 2% concentration, reaching 5.90 J/m², the highest value recorded in the study. However, increasing the CKD content leads to a significant and continuous reduction in fracture energy, with values of 4.04, 3.06, 3.22, and 3.21 J/m² for the 4%, 6%, 8%, and 10% samples, respectively. This decline is likely due to particle agglomeration and poor interfacial bonding at higher filler concentrations, which generate weak zones within the composite structure and reduce its ability to resist crack

propagation. Overall, the results suggest that while both fillers can enhance the fracture performance of epoxy composites, their effectiveness is highly dependent on filler concentration, with optimal results achieved at lower levels for CKD and moderate levels for concrete waste.

3.4 Fracture toughness results

3.4.1 Compact tension (C.T)

Figure 13 presents the effect of incorporating recycled fillers on the fracture toughness of epoxy composites (EP), using the compact tension (CT) test as the evaluation method. The reference sample (pure epoxy) exhibits a fracture toughness 0.204 MPa√m, indicating a moderate resistance to crack initiation and propagation in the absence of reinforcement. Epoxy composites reinforced with concrete waste show a marked improvement in fracture toughness compared to the neat epoxy. The recorded values are as follows 2%: 0.308 MPa√m, 4%: 0.330 MPa√m, 6%: 0.300 MPa√m, 8%: 0.262 MPa√m, 10%: 0.292 MPa√m. The optimum performance is achieved at a filler content of 4%, with a fracture toughness of 0.330 MPa√m, representing an approximate 62% increase over the unmodified epoxy. This enhancement is attributed to the effective dispersion of filler particles within the matrix, which improves toughness and inhibits crack propagation through mechanisms such as crack deflection and energy dissipation. At higher filler contents (6–10%), a slight reduction in fracture toughness is observed, likely due to filler agglomeration or the formation of micro voids, which act as stress concentrators and impair the efficient transfer of mechanical loads.

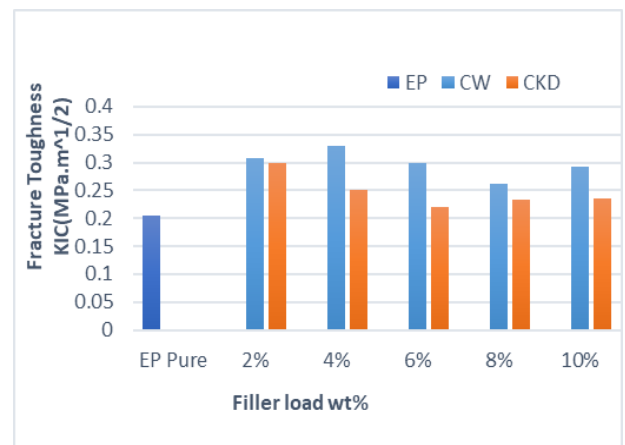


Figure 13. Effect of filler content (w.t%) on the fracture toughness (CT) of the epoxy matrix

Composites containing CKD also exhibit improved fracture toughness at low filler levels, particularly at 2%, after which a gradual decline is noted with increasing filler content. The measured values are 2%: 0.299 MPa√m, 4%: 0.250 MPa√m, 6%: 0.220 MPa√m, 8%: 0.233 MPa√m and 10%: 0.235 MPa√m. The maximum toughness recorded for the CKD-reinforced composites is 0.299 MPa√m at 2% content, indicating a 46.5% improvement over the pure epoxy. This result suggests that CKD can be an effective reinforcement at low concentrations due to its fine particle size and surface characteristics, which may promote mechanical interlocking and energy absorption. However, as the filler ratio increased, the performance declined consistently. This degradation can be attributed to poor dispersion, filler agglomeration, and

weak interfacial adhesion between the CKD particles and the epoxy matrix, leading to the development of structural defects that compromise the material's fracture resistance.

3.4.2 Single edge notched bending (SENB)

Figure 14 represents the relationship between the fracture toughness and the weight percentage of each of the recycled fillers, namely, concrete waste and cement kiln dust (CKD), at ratios of 2%, 4%, 6%, 8%, and 10%. The results show that the fracture toughness of pure epoxy reaches $0.1259 \text{ MPa}\sqrt{\text{m}}$, which serves as the reference value for comparison. With the addition of concrete waste, a significant improvement in fracture toughness is observed, reaching $0.2023 \text{ MPa}\sqrt{\text{m}}$ at 2% and continuing to increase at 4%, demonstrating the effectiveness of the added particles in improving the material's resistance to crack propagation. However, the values gradually decreased at higher ratios, recording $0.198 \text{ MPa}\sqrt{\text{m}}$ at 6% and $0.189 \text{ MPa}\sqrt{\text{m}}$ at 8%. This decline is attributed to the potential for filler agglomerations within the polymer matrix. With CKD as a filler, the highest fracture toughness value is recorded at 2%, reaching $0.1677 \text{ MPa}\sqrt{\text{m}}$, a value higher than that recorded for pure epoxy, indicating an initial improvement in mechanical properties. However, performance deteriorated with increasing addition ratio, decreasing to $0.1514 \text{ MPa}\sqrt{\text{m}}$ at 4% and then increasing slightly at 6%, reaching $0.1559 \text{ MPa}\sqrt{\text{m}}$. This behavior reflects instability in mechanical performance, likely caused by the inhomogeneous distribution of particles within the matrix or the formation of agglomerations that reduce the filler's effectiveness in enhancing fracture toughness.

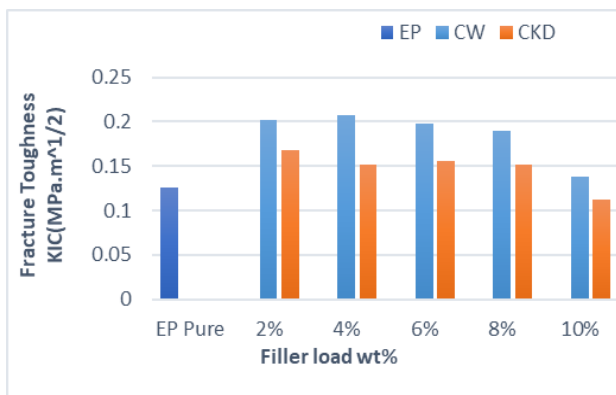


Figure 14. Effect of filler content (w.t%) on the fracture toughness (SENB) of the epoxy matrix

3.5 Pull off adhesion results

The adhesion test results reveal that the unmodified epoxy exhibits an adhesion strength, with a value of 2.88 MPa, as

shown in Figure 15. Upon incorporating recycled concrete waste (CW) as filler, a noticeable improvement is observed, with the adhesion strength rising from 3.56 MPa at 2% to peaking with 5.02 MPa at 6% by weight, compared to pure epoxy. This improvement is attributed to improved mechanical interlocking between the filler particles and the epoxy matrix, which enhances internal cohesion. However, the adhesion strength decreased abruptly at 8% by weight. When cement kiln dust (CKD) was used as a filler, the 2% by weight filler samples recorded the highest bond strength of 6.48 MPa, followed by a gradual decrease to 3.90 MPa at 6%. However, the strength increases again to 5.33 MPa at 8% and reaches 6.07 MPa at 10%. This improvement is attributed to the increased surface roughness of the epoxy upon wetting, which enhances the mechanical interlocking between the microfillers and the substrate surface, as well as the good dispersion of particles within the matrix. In general, all CKD-filled samples demonstrated superior bonding performance compared to pure epoxy. These results confirm that the use of CW and CKD fillers not only contributes to enhanced environmental sustainability and reduced costs but also improves the adhesion properties of epoxy composites when the loading ratios and particle distribution are appropriately adjusted.

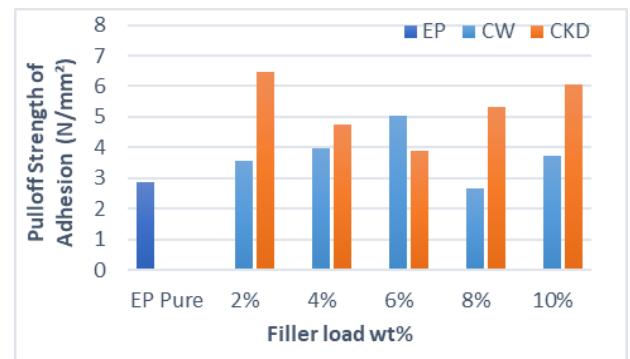


Figure 15. Relationship between adhesion strength and filler loading (wt%)

All images shown in Figure 16 indicate that the failure mode was cohesive failure, where the fracture occurred within the coating or substrate rather than at the bond interface. This type of failure indicates that the bonding strength between the coating and the concrete surface is higher than the bonding strength of the material itself, demonstrating that the coating system used has excellent performance and is considered one of the best coatings for bonding strength. The remains of the concrete substrate bonded to the back of the studs confirm that the adhesive maintained its cohesion, indicating a cohesive failure in the substrate. This type of failure is a positive indicator.



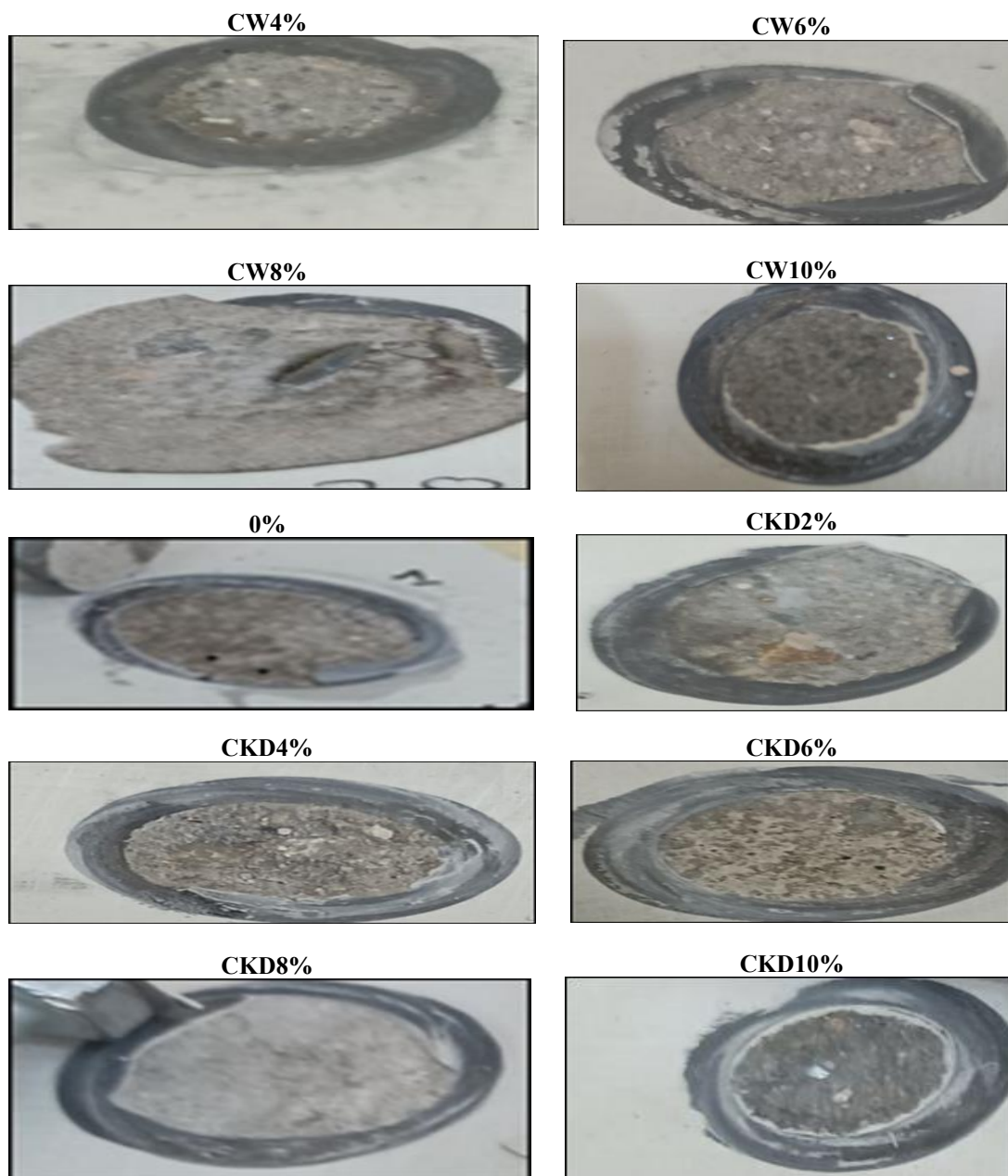


Figure 16. Image illustrating adhesive failure on the surface of the concrete substrate

3.6 FTIR result

The FTIR spectrum of the pure epoxy sample (EP) and the samples filled with concrete waste (CW) and cement kiln dust (CKD) show clear stability in the absorption sites associated with the main functional degrees, as shown in Figure 17, indicating that no chemical interactions occurred between the polymer matrix and the added fillers. The broad absorption peak at $\sim 3400\text{ cm}^{-1}$, attributed to O–H stretching vibrations, appeared in all samples, with minor changes in intensity, suggesting the possible presence of weak surface hydrogen bonds. The aliphatic C–H stretching peak at $\sim 2920\text{ cm}^{-1}$ appeared without significant change, indicating the stability of the molecular chains. The peak at $\sim 1600\text{ cm}^{-1}$, associated with C=C vibrations in the aromatic ring, remained constant, confirming that the aromatic structure of the epoxy was not affected. Furthermore, aromatic C–H bending peaks appeared at $\sim 1500\text{--}1450\text{ cm}^{-1}$, C–O stretching peaks in ether bonds at $\sim 1250\text{--}1150\text{ cm}^{-1}$, and the characteristic asymmetric C–O–C

vibration peak at $\sim 1100\text{ cm}^{-1}$, all of which maintained their relative positions and intensities, indicating no cracking or modification of the polymer network. Finally, out-of-plane C–H vibrations of the aromatic ring at $\sim 870\text{--}750\text{ cm}^{-1}$ appeared consistently across the samples, reinforcing the hypothesis that the interaction between the fillers and the matrix proceeds via physical mechanisms such as surface crosslinking or mechanical cohesion, without the formation of new covalent bonds.

3.7 Scanning electron microscopy (SEM) result

Scanning electron microscope (SEM) analyses reveal the effect of concrete waste (CW) and cement kiln dust (CKD) content on the microstructure of epoxy composites. Pure epoxy was characterized by a smooth, homogeneous surface, indicating an effective three-dimensional network structure as depicted in Figure 18(a). When 2% by weight of both CW and CKD were added as illustrated in Figure 18(b) and (c), even

particle distribution within the matrix was observed, without obvious structural defects, indicating acceptable compatibility between the filler and binder. As the filler content increased to 10% by weight, as shown in Figures 18(d) and (e), the roughness surface becomes higher and clear particle agglomerations, defined joints between the filler and binder,

and indications of poor internal bonding were observed. These results confirm that excessive filler content leads to microstructure complexity, necessitating adjustments in the addition ratios or surface modifications to the particles to ensure effective mechanical performance and structural integrity of the composite.

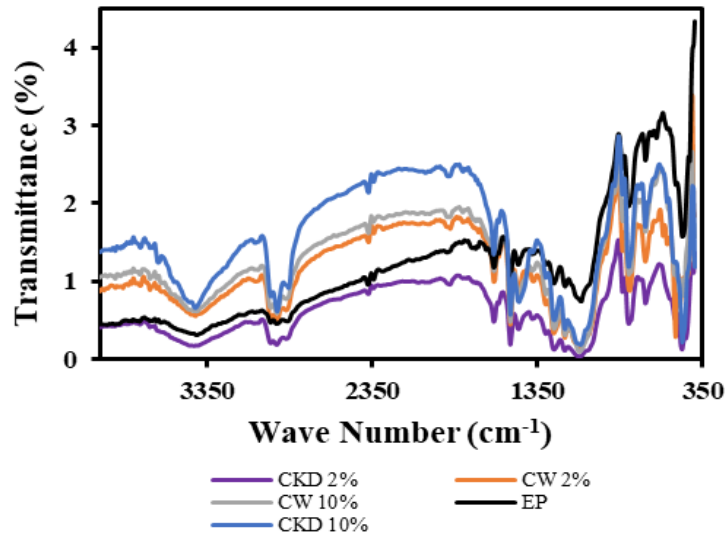


Figure 17. FTIR spectra of pure epoxy, epoxy+ concrete waste (CW2%), (CW10%), and epoxy+ cement kin dust (CKD), (CKD2%, CKD10%)

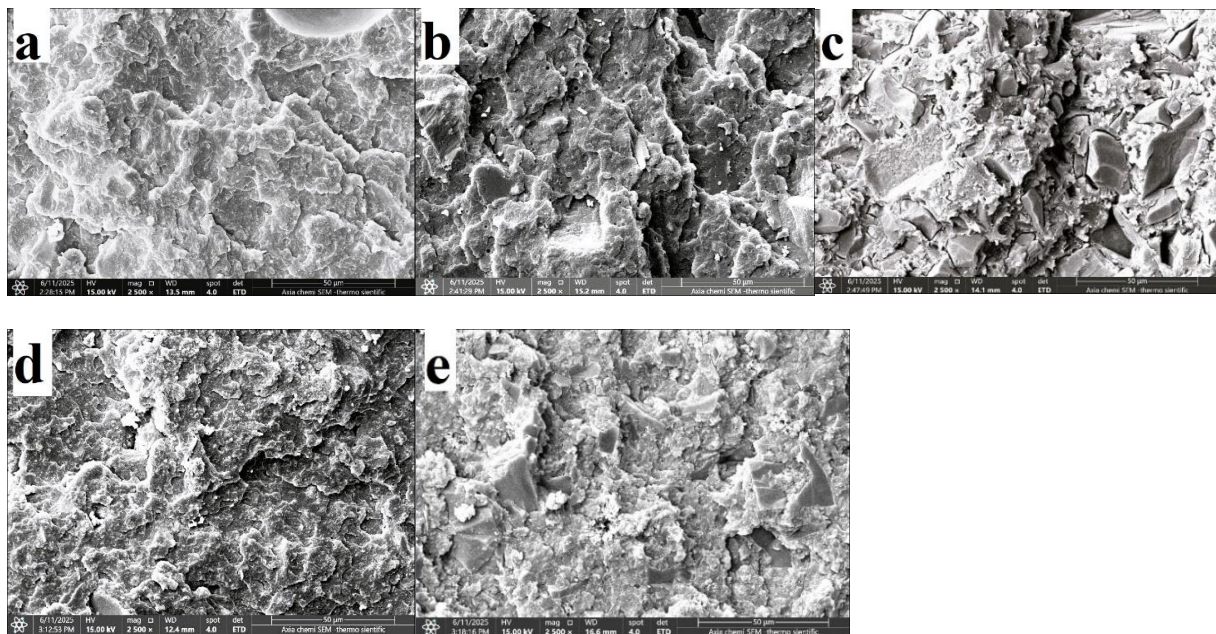


Figure 18. SEM images of the pure epoxy sample with various loading of fillers a) pure epoxy (b) epoxy/CW with 2%wt, (c) epoxy/CW with 10% wt (d) epoxy/CKD with 2% wt and (e) epoxy/CKD with 10% wt

4. CONCLUSION

The results show that reinforcing epoxy with concrete and kiln waste (CKD) improves some mechanical properties only at specific filler ratios. Concrete waste performs best in tensile strength, modulus of elasticity, and fracture toughness at 4–6% filler ratios, due to improved physical bonding and filler distribution. In contrast, CKD shows limited improvement in tensile strength and modulus of elasticity, but the hardness test results show that the combination of CW and CKD did not

significantly affect the hardness of the epoxy when recycled materials were added. This is attributed to the physical bonding. Adhesion test results indicate that moderate filler loading promotes mechanical interlocking and improves performance, while overloading leads to particle agglomeration and poor bonding; however, all CKD samples demonstrated clear superiority over unmodified epoxy in terms of adhesion strength. FTIR analysis reveals surface physical interactions without any change in the basic chemical composition of the epoxy, while SEM images reveal that

increasing the filler content leads to elevated surface roughness, primarily due to the agglomeration and clustering of microparticles resulting from poor dispersion. These morphological features are accompanied by signs of weak internal bonding, which negatively impact the mechanical properties of the composite.

REFERENCES

- [1] Ncube, L.K., Ude, A.U., Ogunmuyiwa, E.N., Zulkifli, R., Beas, I.N. (2021). An overview of plastic waste generation and management in food packaging industries. *Recycling*, 6(1): 12. <https://doi.org/10.3390/recycling6010012>
- [2] Koblischek, P.J. (1990). Protection of surfaces of natural stone and concrete through polymers. *Surface Engineering*, 62-71. https://doi.org/10.1007/978-94-009-0773-7_7
- [3] Klose, L., Meyer-Heydecke, N., Wongwattanasat, S., Chow, J., et al. (2023). Towards sustainable recycling of epoxy-based polymers: Approaches and challenges of epoxy biodegradation. *Polymers*, 15(12): 2653. <https://doi.org/10.3390/polym15122653>
- [4] Chowaniec, A. (2021). Using waste limestone powder as filler in a toxic epoxy resin coating and its influence on adhesive properties. *Chemical Engineering Transactions*, 88: 1063-1068. <https://doi.org/10.3303/CET2188177>
- [5] Chowaniec, A., Sadowski, Ł., Żak, A. (2020). The chemical and microstructural analysis of the adhesive properties of epoxy resin coatings modified using waste glass powder. *Applied Surface Science*, 504: 144373. <https://doi.org/10.1016/j.apsusc.2019.144373>
- [6] Bolden IV, J.J. (2013). Innovative Uses of Recycled and Waste Materials in Construction Application. North Carolina Agricultural and Technical State University.
- [7] Almusallam, A.F.M.K., Khan, F.M., Maslehuddin, M. (2002). Performance of concrete coating under varying exposure conditions. *Materials and Structures*, 35(8): 487-494. <https://doi.org/10.1007/BF02483136>
- [8] Szweczek, A., Łagód, G. (2022). Adhesion of modified epoxy resin to a concrete surface. *Materials*, 15(24): 8961. <https://doi.org/10.3390/ma15248961>
- [9] Hodul, J., Mészárosová, L., Drochytka, R. (2021). Recovery of industrial wastes as fillers in the epoxy thermosets for building application. *Materials*, 14(13): 3490. <https://doi.org/10.3390/ma14133490>
- [10] Ağcan, A.E., Kartal, İ. (2025). A review of waste-derived fillers for enhancing the properties of epoxy resins. *International Journal of Adhesion and Adhesives*, 138: 103944. <https://doi.org/10.1016/j.ijadhadh.2025.103944>
- [11] Zhao, H., Wang, Q., Shang, R., Li, S. (2025). Development, challenges, and applications of concrete coating technology: Exploring paths to enhance durability and standardization. *Coatings*, 15(4): 409. <https://doi.org/10.3390/coatings15040409>
- [12] Liu, J., Vipulanandan, C. (2005). Tensile bonding strength of epoxy coatings to concrete substrate. *Cement and Concrete Research*, 35(7): 1412-1419. <https://doi.org/10.1016/j.cemconres.2004.06.035>
- [13] Arulrajah, A., Mohammadinia, A., D'Amico, A., Horpibulsuk, S. (2017). Cement kiln dust and fly ash blends as an alternative binder for the stabilization of demolition aggregates. *Construction and Building Materials*, 145: 218-225. <https://doi.org/10.1016/j.conbuildmat.2017.04.007>
- [14] Bal, P. K. (2014). Thermal conductivity of cement kiln dust filled epoxy composites (Doctoral dissertation).
- [15] Alsaadi, Z., Alobad, Z.K., Akraa, M.A. (2024). Effect of modification with polyether polyol and liquid silicon rubber on the mechanical properties of epoxy system. *Kufa Journal of Engineering*, 15(3). <https://doi.org/10.30572/2018/KJE/150310>
- [16] Mohammed, Z.M., Al-Obad, Z.K.M. (2023). Producing low-cost adhesives for concrete applications. 4th International Scientific Conference of Engineering Sciences and Advances Technologies, 2830(1): 030013. <https://doi.org/10.1063/5.0157050>
- [17] ISO 75-1. (2020). Plastics — Determination of temperature of deflection under load. Part 1: General test method. <https://www.iso.org/standard/77576.html?browse=ics>.
- [18] Chowaniec-Michalak, A., Czarnecki, S., Sadowski, Ł., Królicka, A. (2022). Recycling of waste limestone powders for the cleaner production of epoxy coatings: Fundamental understanding of the mechanical and microstructural properties. *Journal of Cleaner Production*, 372: 133828. <https://doi.org/10.1016/j.jclepro.2022.133828>
- [19] ASTM D2240-15. (2017). Standard test methods for rubber property—Durometer hardness. <https://store.astm.org/d2240-15.html>.
- [20] ISO. 179-Part-2. (2020). Plastics — Determination of Charpy impact properties. Part 2: Instrumented impact test. <https://www.iso.org/standard/75825.html>.
- [21] Yang, Z., Peng, H., Wang, W., Liu, T. (2010). Crystallization behavior of poly (ϵ -caprolactone)/layered double hydroxide nanocomposites. *Journal of Applied Polymer Science*, 116(5): 2658-2667. <https://doi.org/10.1002/app.31787>
- [22] ASTM D5045-9. (2007). Standard test methods for plane-strain fracture toughness and strain energy release rate of plastic materials. <https://store.astm.org/d5045-99r07e01.html>.
- [23] Saeed, A.Q., Al-Obad, Z.K.M. (2023). Effect of magnesium oxide, boron nitride, and hybrid nanoparticles on the mechanical properties of epoxy nanocomposites. 4th International Scientific Conference of Engineering Sciences and Advances Technologies, 2830(1): 030036. <https://doi.org/10.1063/5.0157176>
- [24] ASTM, A. (2014). D4541-09: Standard test method for pull-off strength of coatings using portable adhesion. *ASTM Int*, 1-16. <https://store.astm.org/d4541-09.html>.
- [25] Mira, J.B., Restrepo, V., Vajipeyajula, B., Patterson, A.E. (2024). Impact of compact tension specimen size on fracture toughness of FFF-processed thermoplastics. *Procedia Structural Integrity*, 61: 156-163. <https://doi.org/10.1016/j.prostr.2024.06.021>
- [26] ASTM E1252-98. (2021). Standard practice for general techniques for obtaining infrared spectra for qualitative analysis. <https://store.astm.org/e1252-98r21.html>.